Oxalate and 2,2′-Bipyrimidine as Useful Tools in Designing Layered Compounds

Giovanni De Munno,*[1a] Rafael Ruiz,[1b] Francesc Lloret,[1b] Juan Faus,[1b] Roberta Sessoli,[1c] and Miguel Julve*[1b]

Dipartimento di Chimica, Università della Calabria, 87030 Arcavacata di Rende, Cosenza, Italy, Department de Química Inorgànica, Facultat de Química de la Universitat de València, Dr. Moliner 50, 46100 Burjassot, València, Spain, and Dipartimento di Chimica Inorganica, Università degli Studi di Firenze, Via Maragliano 77, 50144 Firenze, Italy

Received March 16, 1994

Special attention has been devoted to the coordination chemistry of ligands such as oxalate and 2,2′-bipyrimidine (hereafter noted ox and bpm, respectively) in the context of magnetostructural studies.[2,3] This interest is mainly based on two features: (i) the design of both mono- and polynuclear species becomes easier when chelating and bischelating ligands such as ox and bpm are used; (ii) these bridging ligands have a remarkable ability to mediate strong exchange interactions between metal ions separated by more than 5 Å. Oxalato-bridged homo- and heteropolynuclear complexes are examples of species wherein tunable exchange can be accomplished by varying the nature of the terminal ligands[2a,b] and the nature of the atoms of the bridge,[2d] high-spin molecules because of strict orthogonality between nearest neighbor magnetic centers,[2e] one-dimensional magnetic chains,[2c] and more recently molecular-based ferromagnets.[2g] As far as bpm-containing metal complexes are concerned, the most interesting results are the easy preparation of dimers with a large variety of transition metal ions,[3a,b] the controlled polymerization from the mononuclear complex to the *n*D network ($n = 1-3$),[3c-f] and the rational design of 1D structures with alternating ferro- and antiferromagnetic interactions.[3g]

In a recent communication,[4] we showed that the reaction of copper(II) with the mononuclear mixed-ligand complex $[Cu(bpm)(ox)(H_2O)_2]\cdot 5H_2O$ yielded the novel 2D compound of formula $[Cu_2(bpm)(ox)_2]\cdot 5H_2O$ where bpm and ox act as bridging ligands. In order to investigate the possibility of extending the preparation of this kind of layered material to that of complexes with other metal ions and establishing the basis of a new strategy aimed at designing magnetic layered compounds, we have undertaken a systematic study of complex formation with first-row transition metal ions and bpm and ox as ligands. In this contribution we present the isolation and the structural and magnetic characterization of the dinuclear complex $[Mn_2(bpm)(H_2O)_4(SO_4)_2]$ (**1**) and the novel sheetlike polymeric compound $[Mn_2(bpm)(ox)_2]\cdot 6H_2O$ (**2**).

Table 1. Crystallographic Data for $[Mn_2(bpm)(H_2O)_6(SO_4)_2]$ (**1**) and $[Mn_2(bpm)(ox)_2]\cdot 6H_2O$ (**2**)

	1	**2**
chem formula	$C_8H_{18}N_4Mn_2O_{14}S_2$	$C_{12}H_{18}N_4Mn_2O_{14}$
a, Å	6.565(2)	6.072(2)
b, Å	13.252(2)	17.628(2)
c, Å	11.100(3)	9.750(2)
β, deg	94.36(2)	101.94(2)
Z	2	2
fw	568.3	552.2
space group	$P2_1/n$	$P2_1/c$
T, K	298	298
λ, Å	0.710 73	0.710 73
ϱ_{calcd}, g cm^{-3}	1.960	1.796
μ, cm^{-1}	15.44	13.17
R^a	0.0496	0.0342
$R_w{}^b$	0.0638	0.0387

$^a R = \sum(|F_o| - |F_c|)/\sum|F_o|$. $^b R_w = [\sum(|F_o| - |F_c|)^2/\sum wF_o^2]^{1/2}$.

Experimental Section

Materials. 2,2′-Bipyrimidine, manganese(II) sulfate hydrate, and sodium oxalate were purchased from commercial sources and used as received. Elemental analyses (C, H, N) were conducted by the Microanalytical Service of the Università degli Studi della Calabria.

Preparation of $[Mn_2(bpm)(H_2O)_4(SO_4)_2]$ (1) and $[Mn_2(bpm)(ox)_2]\cdot 6H_2O$ (2). Compound **1** was obtained as pale yellow polyhedral crystals by slow evaporation of aqueous solutions containing stoichiometric amounts of manganese(II) sulfate and bpm. They were filtered off, washed with cold water and ethanol, and stored under calcium chloride. Orange-yellow polyhedral single crystals of compound **2** were grown from aqueous solutions containing compound **1** and small amounts of sodium oxalate They were filtered off and dried on filter paper. Anal. Calcd for $C_8H_{18}Mn_2N_4O_{14}S_2$ (**1**): C, 16.91; H, 3.17; N, 9.86; S, 11.29. Found: C, 16.82; H, 3.04; N, 9.75; S, 10.77. Calcd for $C_{12}H_{18}Mn_2N_4O_{14}$ (**2**): C, 26.11; H, 3.26; N, 10.14. Found: C, 26.02; H, 3.15; N, 9.98.

Magnetic Susceptibility Measurements. These measurements for compounds **1** and **2** were carried out in the temperature range 3−300 K in a field of 1 T by using a Metronique Ingenierie MS03 SQUID magnetometer. The corrections for the diamagnetism using Pascal's constants are -260×10^{-6} and -256×10^{-6} cm^3 mol^{-1} for complexes **1** and **2**, respectively.

X-ray Data Collection and Structure Refinement. Diffraction data were collected at room temperature on a Siemens R3m/V automatic diffractometer by using graphite-monochromatized Mo Kα radiation and the ω-2θ scan technique. Unit cell dimensions and crystal orientation matrices were obtained from least-squares refinement of 25 strong reflections in the $15 \le \theta \le 30°$ range. A summary of the crystallographic data and structure refinement is given in Table 1. A more complete list of crystallographic data is reported in Table S1.[5] Totals of 2508 (**1**) and 2582 (**2**) reflections were collected in the ranges $3 \le \theta \le 55°$ (**1**) and $3 \le \theta \le 54°$ (**2**); 2216 (**1**) and 2241 (**2**) of them were unique, and from these, 1913 (**1**) and 1557 (**2**) were assumed as observed ($I > 3\sigma(I)$). Examination of three standard reflections, monitored after every 100, showed no sign of crystal deterioration. Lorentz-polarization and ψ scan absorption corrections[6] were applied to the intensity data. The maximum and minimum transmission factors were 0.524 and 0.404 for **1** and 0.811 and 0.729 for **2**.

(1) (a) Università della Calabria. (b) Universitat de València. (c) Università di Firenze.
(2) (a) Felthouse, T. R.; Laskowski, E. J.; Hendrickson, D. N. *Inorg. Chem.* **1977**, *16*, 1077. (b) Julve, M.; Verdaguer, M.; Kahn, O.; Gleizes, A.; Philoche-Levisalles, M. *Inorg. Chem.* **1983**, *22*, 368; **1984**, *23*, 3808. (c) Verdaguer, M.; Julve, M.; Michalowicz, A.; Kahn, O. *Inorg. Chem.* **1983**, *22*, 2624. (d) Verdaguer, M.; Kahn, O.; Julve, M.; Gleizes, A. *Nouv. J. Chim.* **1985**, *9*, 325. (e) Pei, Y.; Journaux, Y.; Kahn, O. *Inorg. Chem.* **1989**, *28*, 100. (f) Alvarez, S.; Julve, M.; Verdaguer, M. *Inorg. Chem.* **1990**, *29*, 4500. (g) Tamaki, H.; Zhong, Z. J.; Matsumoto, N.; Kida, S.; Koikawa, M.; Achiva, N.; Hashimoto, Y.; Okawa, H. *J. Am. Chem. Soc.* **1992**, *114*, 6974.
(3) (a) Brewer, G.; Sinn, E. *Inorg. Chem.* **1985**, *24*, 4580. (b) Andrés, E.; De Munno, G.; Julve, M.; Real, J. A.; Lloret, F. *J. Chem. Soc., Dalton Trans.* **1993**, 2169. (c) Julve, M.; De Munno, G.; Bruno, G.; Verdaguer, M. *Inorg. Chem.* **1988**, *27*, 3160. (d) Morgan, L. W.; Goodwin, K. V.; Pennington, W. T.; Petersen, J. D. *Inorg. Chem.* **1992**, *31*, 1103. (e) De Munno, G.; Julve, M.; Verdaguer, M.; Bruno, G. *Inorg. Chem.* **1993**, *32*, 2215. (f) Julve, M.; Verdaguer, M.; De Munno, G.; Real, J. A.; Bruno, G. *Inorg. Chem.* **1993**, *32*, 795. (g) De Munno, Julve, M.; Lloret, F.; Faus, J.; Verdaguer, M.; Caneschi, A. *Angew. Chem., Int. Ed. Engl.* **1993**, *32*, 1046.
(4) De Munno, G.; Julve, M.; Nicoló, F.; Lloret, F.; Faus, J.; Ruiz, R.; Sinn, E. *Angew. Chem., Int. Ed. Engl.* **1993**, *32*, 613.
(5) Supplementary material.
(6) North, A. C. T.; Philips, D. C.; Mathews, F. S. *Acta Crystallogr.* **1968**, *A24*, 351.

0020-1669/95/1334-0408$09.00/0

Table 2. Final Atomic Fractional Coordinates and Equivalent Isotropic Displacement Parameters[a,b] for Non-Hydrogen Atoms of Complex **1**

atom	x/a	y/b	z/c	10^3U_{eq}, Å^2
Mn(1)	0.0527(1)	0.0477(1)	0.2704(1)	28(1)
O(1)	−0.1228(6)	0.1868(2)	0.2406(3)	48(1)
O(2)	0.2097(5)	−0.0965(3)	0.2904(3)	48(1)
O(3)	0.1679(5)	0.0027(3)	0.3927(3)	41(1)
N(1)	0.1887(4)	0.0731(2)	0.0881(3)	27(1)
C(1)	0.3571(6)	0.1257(3)	0.0697(3)	36(1)
C(2)	0.4335(6)	0.1329(3)	−0.0428(4)	39(1)
C(3)	0.3270(6)	0.0831(3)	−0.1362(3)	35(1)
N(2)	0.1574(5)	0.0302(2)	−0.1198(3)	26(1)
C(4)	0.0954(5)	0.0285(2)	−0.0086(3)	22(1)
S(1)	0.4175(1)	0.1850(1)	0.4343(1)	27(1)
O(4)	−0.2712(9)	0.1110(3)	0.3920(4)	112(2)
O(5)[c]	0.6066(8)	0.1415(4)	0.4916(4)	49(2)
O(6)[c]	0.3376(1)	0.2536(9)	0.5125(6)	124(4)
O(7)[c]	0.4812(1)	0.2379(5)	0.3251(5)	72(2)
O(5′)[d]	0.3781(59)	0.1775(9)	0.5583(10)	177(17)
O(6′)[d]	0.3763(14)	0.2849(6)	0.3939(8)	29(2)
O(7′)[d]	0.5800(39)	0.1452(16)	0.3883(36)	191(17)

[a] Estimated standard deviations in the last significant digits are given in parentheses. [b] U values for anisotropically refined atoms are given in the form of the isotropic equivalent thermal parameter $U_{eq} = {}^1/_3(U_{11} + U_{22} + U_{33})$. [c] Atoms with a population parameter 0.7. [d] Atoms with a population parameter 0.3.

The structures of compounds **1** and **2** were solved by standard Patterson methods with the SHELXTL PLUS program[7] and subsequently completed by Fourier recycling. On the difference map of compound **1**, several sulfate oxygen positions were localized because of different coexistent orientations of the sulfate group. This disorder was described by assigning population parameters of 0.7 and 0.3 to each pair of sites. All non-hydrogen atoms were refined anisotropically. The hydrogen atoms of the water molecules were located on a ΔF map and refined with constraints. The hydrogen atoms of bpm were set in calculated positions and refined as riding atoms. A common thermal parameter was assigned to these atoms. The final full-matrix least-squares refinement, minimizing the function $\sum w(|F_o| - |F_c|)^2$ with $w = 1/[\sigma^2(F_o) + q(F_o)^2]$ ($q = 0.0010$ for **1** and 0.0007 for **2**), converged to final residuals R (R_w) of 0.0496 (0.0638) for **1** and 0.0342 (0.0387) for **2**. The goodness of fit values were 2.260 (**1**) and 1.244 (**2**). In the final difference map residual maxima and minima were 1.15 and −0.85 e Å^{-3} for **1** and 0.41 and −0.37 e Å^{-3} for **2**. All calculations were performed on a micro-Vax II computer, using the SHELXTL-PLUS system. The final geometrical calculations and graphical manipulations were carried out with the PARST program[8] and XP utility of the SHELXTL-PLUS system, respectively. Final fractional coordinates are gathered in Tables 2 (**1**) and 3 (**2**); selected bond distances and angles, in Tables 4 (**1**) and 5 (**2**). Anisotropic thermal parameters, hydrogen atom coordinates, intramolecular bond distances and angles, hydrogen-bond parameters, and least-squares planes are given in the supplementary material.

Results and Discussion

Description of the Structures. $[Mn_2(bpm)(H_2O)_4(SO_4)_2]$ (1). The crystal structure of **1** is composed of neutral bpm-bridged manganese(II) dimers of formula $[Mn_2(bpm)(H_2O)_4(SO_4)_2]$ with a crystallographically imposed inversion center located halfway between the halves of the bpm molecule. The molecular geometry and the atom-numbering scheme for **1** are shown in Figure 1. **1** is isostructural with the parent $[Fe_2(bpm)(H_2O)_4(SO_4)_2]$.[3b] Each manganese atom is hexacoordinate: two nitrogen atoms from bpm and four oxygen atoms, three of them from water molecules and the remaining one from a monodentate sulfato ligand, form a distorted octahedron around the metal atom. The Mn−N bond distances (average value 2.313(3) Å) are significantly longer than the Mn−O distances (average value 2.143(3) Å) and that involving coordinated sulfate is the shortest (2.070(5) Å for Mn(1)−O(4)). The best equatorial plane is defined by the atoms N(1), N(2a), O(3), and O(4) (the largest deviation from the mean plane is 0.109(5) Å at O(4)), and the manganese atom is only 0.002(1) Å out of this plane. The dihedral angle between the bpm and equatorial N(1)N(2a)O(3)O(4) mean planes is 4.9(1)°. A comparison of **1** with the parent bpm-bridged iron(II),[3b] nickel(II),[9a] and cobalt(II)[3a,9b] dinuclear compounds reveals that the present manganese(II) complex exhibits the largest metal−metal separation through

Table 3. Final Atomic Fractional Coordinates and Equivalent Isotropic Displacement Parameters[a,b] for Non-Hydrogen Atoms of Complex **2**

atom	x/a	y/b	z/c	10^3U_{eq}, Å^2
Mn(1)	0.4984(1)	0.1714(1)	0.0164(1)	29(1)
N(1)	0.7069(4)	0.0658(1)	0.0890(2)	28(1)
C(1)	0.9151(5)	0.0642(2)	0.1693(3)	35(1)
C(2)	1.0286(5)	−0.0033(2)	0.2020(3)	38(1)
C(3)	0.9218(5)	−0.0690(2)	0.1521(3)	35(1)
C(4)	0.6150(4)	−0.0009(2)	0.0449(3)	23(1)
N(2)	0.7109(4)	−0.0681(1)	0.0720(3)	26(1)
O(1)	0.7020(4)	0.1911(1)	−0.1370(2)	38(1)
O(2)	0.2953(4)	0.2479(1)	−0.1308(2)	36(1)
C(5)	0.6189(5)	0.2345(2)	−0.2340(3)	29(1)
C(6)	0.3828(5)	0.2680(2)	−0.2309(3)	28(1)
O(3)	0.7059(3)	0.2545(1)	−0.3339(2)	36(1)
O(4)	0.2976(3)	0.3118(1)	−0.3279(2)	37(1)
O(5)	1.0102(5)	0.1734(2)	−0.4766(3)	70(1)
O(6)	0.6426(6)	0.0815(2)	−0.5826(4)	90(2)
O(7)	1.3752(6)	0.0723(2)	−0.3847(4)	92(2)

[a] Estimated standard deviations in the last significant digits are given in parentheses. [b] U values for anisotropically refined atoms are given in the form of the isotropic equivalent thermal parameter $U_{eq} = {}^1/_3(U_{11} + U_{22} + U_{33})$.

Table 4. Selected Bond Lengths (Å) and Interbond Angles (deg) for Complex **1**[a]

	Distances		
Mn(1)−O(1)	2.185(3)	Mn(1)−O(4)	2.070(5)
Mn(1)−O(2)	2.175(3)	Mn(1)−N(1)	2.298(3)
Mn(1)−O(3)	2.143(3)	Mn(1)−N(2a)	2.327(3)
	Angles		
N(1)−Mn(1)−N(2a)	71.4(1)	N(2a)−Mn(1)−O(2)	86.2(1)
N(1)−Mn(1)−O(3)	157.7(1)	O(3)−Mn(1)−O(4)	99.7(2)
N(1)−Mn(1)−O(4)	102.6(2)	O(3)−Mn(1)−O(1)	87.5(1)
N(1)−Mn(1)−O(1)	88.8(1)	O(3)−Mn(1)−O(2)	91.6(7)
N(1)−Mn(1)−O(2)	90.3(1)	O(4)−Mn(1)−O(1)	95.1(2)
N(2a)−Mn(1)−O(3)	86.5(1)	O(4)−Mn(1)−O(2)	89.4(2)
N(2a)−Mn(1)−O(4)	172.5(2)	O(1)−Mn(1)−O(2)	175.5(1)
N(2a)−Mn(1)−O(1)	89.3(1)		

[a] Symmetry code: (a) $-x, -y, -z$.

Table 5. Selected Bond Lengths (Å) and Interbond Angles (deg) for Complex **2**[a]

	Distances		
Mn(1)−O(1)	2.157(2)	Mn(1)−O(4f)	2.155(2)
Mn(1)−O(2)	2.160(2)	Mn(1)−N(1)	2.280(2)
Mn(1)−O(3f)	2.159(2)	Mn(1)−N(2a)	2.285(2)
	Angles		
N(1)−Mn(1)−N(2a)	72.3(1)	N(2a)−Mn(1)−O(4f)	91.3(1)
N(1)−Mn(1)−O(2)	156.9(1)	O(2)−Mn(1)−O(3f)	104.1(1)
N(1)−Mn(1)−O(3f)	94.3(1)	O(2)−Mn(1)−O(1)	76.7(1)
N(1)−Mn(1)−O(1)	89.2(1)	O(2)−Mn(1)−O(4f)	93.1(1)
N(1)−Mn(1)−O(4f)	104.6(1)	O(3f)−Mn(1)−O(1)	91.9(1)
N(2a)−Mn(1)−O(2)	92.9(1)	O(3f)−Mn(1)−O(4f)	77.1(1)
N(2a)−Mn(1)−O(3f)	159.8(1)	O(1)−Mn(1)−O(4f)	162.8(1)
N(2a)−Mn(1)−O(1)	102.7(1)		

[a] Symmetry codes: (a) $1-x, -y, -z$; (f) $x, y, {}^1/_2 + z$.

(7) *SHELXTL-PLUS*, Version 4.11/V; Siemens Analytical X-Ray Instruments Inc.: Madison, WI, 1990.
(8) Nardelli, M. *Comput. Chem.* **1983**, *7*, 95.

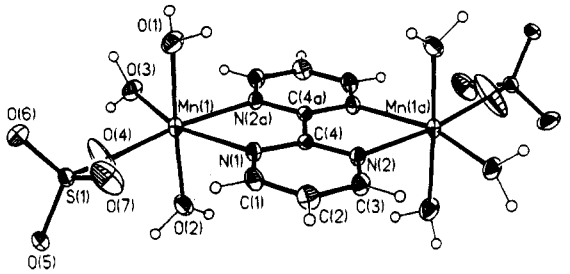

Figure 1. Perspective drawing of **1** (ellipsoids drawn at the 30% probability level) with the labeling scheme. Symmetry code: (a) $-x$, $-y$, $-z$.

the bridging bpm (6.123(2) Å for Mn(1)···Mn(1a)) and the smallest bite bpm angle (71.4(1)° for N(1)−Mn(1)−N(2a)). The lengthening of the metal−nitrogen bonds upon going from Ni to Mn accounts for these structural features. The dinuclear units of **1** are held together by hydrogen bonds involving coordinated water and sulfato groups (two equivalent hydrogen bonds involving O(3) and O(4f) and involving O(4) and O(3f); symmetry code (f) $-x$, $-y$, $1-z$) to yield a one-dimensional arrangement of dimers, the resulting interdimer Mn(1)···Mn(1f) separation being 5.347(2) Å.

$[Mn_2(bpm)(ox)_2]\cdot 6H_2O$ (2). The crystal structure of **2** consists of a 2D array of manganese atoms bridged by bischelating oxalato and bpm groups as shown in Figure 2. The metal atom is in a distorted octahedral MnN_2O_4 environment as in the preceding structure. This compound is very similar to the parent copper(II) complex of formula $[Cu_2(bpm)(ox)_2]\cdot 5H_2O$ (**3**).[4] A lengthening of all bonds around the metal atom is observed in **2** with respect to **3** with the consequent decrease of the oxalato and bpm bite angles. The average values of the Mn−O(ox) and Mn−N(bpm) equatorial distances increase from 2.086(3) and 2.129(3) Å in **3** to 2.160(2) and 2.283(2) Å in **2**. Analogously, the average Mn−O(ox) axial distance increases from 2.076(3) in **3** to 2.156(2) Å in **2**. As a consequence of the geometrical variations around the metal atom, larger hexameric rings occur in **2** with respect to **3**. The pyrimidyl rings of bpm in both compounds **1** and **2** are planar as in the ligand as a whole. The oxalate group is also planar. Bond distances and angles within the bischelating bpm in **1** and **2** and bridging oxalate in **2** are in agreement with those reported in the literature. The intra-ring carbon−carbon bond distance in bpm (1.487(7) and 1488(5) Å in **1** and **2**, respectively) is significantly shorter than the carbon−carbon bond length in the oxalato ligand (1.557(4) Å). The dihedral angle between bpm and oxalato planes is 78.6(1)°. The manganese atom is slightly out of the bpm and oxalate planes [0.066(1) and −0.011(1) Å, respectively]. The intra-ring Mn···Mn distances are 6.052(1), 5.608(1), 10.233(1), 11.748(1), 9.750(1), and 11.590(1) Å for Mn(1)···Mn(1a), Mn(1)···Mn(1e), Mn(1)···Mn(1b), Mn(1)···Mn(1c), Mn(1)···Mn(d), and Mn(1b)···Mn(1e), respectively. Six water molecules (there were five in **3**) are located in each hole of the sheetlike polymer and are linked by hydrogen bonds to form a planar six-membered ring [the maximum deviation from the mean plane is 0.037(4) Å at O(6)].[10] This plane and that

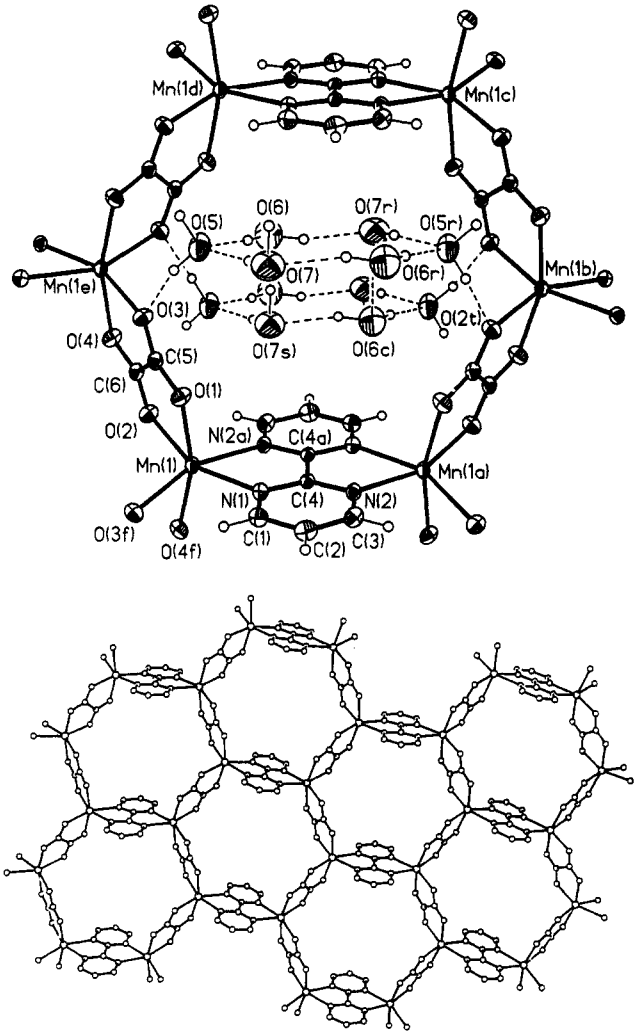

Figure 2. View of the structure of **2** (ellipsoids at the 30% probability level): (top) hexameric repeating unit with the labeling scheme; (bottom) a sheet of **2** extending in the xz plane that shows the chicken-wire arrangement adopted by the manganese atoms (hydrogen atoms and water molecules have been omitted for the sake of clarity). Symmetry codes: (a) $1-x, -y, -z$; (b) $1-x, -1/2+y, -1/2-z$; (c) $1-x, -y, -1-z$; (d) $x, y, -1+z$; (e) $x, 1/2-y, -1/2+z$; (f) $x, y, 1/2+z$; (r) $2-x, -y, -1-z$; (t) $1-x, 1/2+y, -1/2-z$; (s) $-1+x, y, z$.

of bpm form a dihedral angle of 9.5(1)°. The layers of the polymer are stacked by graphite interactions between the bpm rings [the shortest carbon−carbon separation between bpm of parallel layers is 3.448(3) Å].

Magnetic Properties. The thermal dependence of the molar magnetic susceptibility χ_M of complex **1** is characteristic of an antiferromagnetic interaction between the two single-ion sextuplet states: the value of χ_M at room temperature is in the range expected for two $S = 5/2$ states ($\chi_M T = 8.18$ cm^3 mol^{-1} K versus a calculated value of 8.75 cm^3 mol^{-1} K for two uncoupled high-spin Mn(II) ions), increases as the temperature is lowered until a maximum is reached ($T_{max} = 4.5$ K), and finally decreases. The susceptibility of **1** was successfully analyzed in terms of an isotropic exchange interaction for a dinuclear species with $H = -JS_1 \cdot S_2$ with $S_1 = S_2 = 5/2$. Least-squares analysis for **1** yielded $J = -1.1$ cm^{-1} and $g = 1.98$ with $R = 6.0 \times 10^{-5}$ (R is the agreement factor defined as $\Sigma(\chi_M^{obsd} - \chi_M^{calcd})^2/\Sigma(\chi_M^{obsd})^2$). This value is practically identical to that previously reported for another bpm-bridged manganese(II) dimer[3a] whose structure is unknown. The thermal variation of the molar magnetic susceptibility of complex **2** in the form of a χ_M versus

(9) (a) De Munno, G.; Julve, M.; Lloret, F.; Derory, A. *J. Chem. Soc., Dalton Trans.* **1993**, 1179. (b) De Munno, G.; Julve, M.; Lloret, F.; Faus, J.; Caneschi, A. *J. Chem. Soc., Dalton Trans.*, **1994**, 1175.

(10) Within the water ring, O(6) and O(6r) water molecules donate two H atoms, those of O(7) and O(7r) donate only one H atom, and O(5) acts as acceptor. Extensive hydrogen bonding occurs between these six-membered rings which are inserted into the channels delimited by the cavities along the x direction. The water rings are also anchored to the wall of the channel through hydrogen bonds involving O(5) and O(5r) water molecules and O(3) and O(2t) oxalate oxygens.

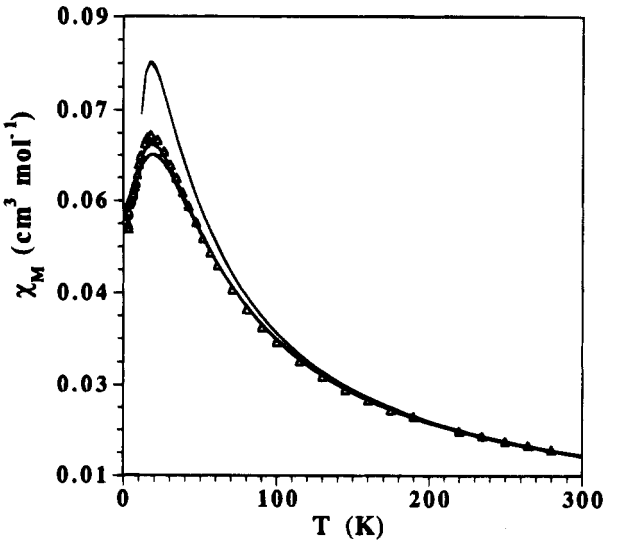

Figure 3. Thermal dependence of the magnetic susceptibility χ_M per two manganese atoms for complex **2**: (△) experimental data; (—) theoretical curves for a honeycomb Heisenberg 2D lattice (top), a Heisenberg type chain model with interchain interactions (middle), and an isolated Heisenberg type chain (bottom) with $S = {}^5/_2$ (see text).

T plot is depicted in Figure 3. $\chi_M T$ exhibits a continuous decrease upon cooling with $\chi_M T = 8.35$ cm^3 mol^{-1} K at 290 K and an extrapolated value that vanishes when T approaches zero. The maximum in the susceptibility curve of **2** is at 18 K. As for **1**, this curve is characterstic of antiferromagnetically coupled high-spin Mn(II)ions. In this compound, exchange pathways through bpm and ox are possible. In this regard, a value of -2.4 cm^{-1} has been reported for the exchange coupling between Mn(II) ions through oxalato ligands Mn(bpy)(ox)[11] (**4**) (bpy = 2,2′-bipyridine) chain. It should be noted that the environment of Mn(II) in **1** and **4** is the same as that in **2** (MnN_2O_4 chromophore). Therefore, the values of the exchange coupling through bpm in **1** and through ox in **4** could be expected in **2**. These data strongly suggest the occurrence of alternating antiferromagnetic interactions through bpm and ox in **2**, the alternating parameter being close to 0.5. The lack of a theoretical law for such an alternating magnetic plane has precluded a detailed analysis of its magnetic behavior. Attempts to fit the magnetic dat of **2** to a honeycomb Heisenberg 2D lattice[12] and a Heisenberg type chain[13] with $S = {}^5/_2$ lead to bad fits. However, the magnetic behavior of **2** is closer to that of the chain model. So a good fit is achieved when interchain interactions (Θ) are considered in the Heisenberg type chain expression (middle curve as continuous line in Figure 3): the values of J, g, θ, and R are -3.0 cm^{-1}, 1.99, -0.2 cm^{-1}, and 3.4×10^{-4}, respectively. The theoretical curves for a honeycomb Heisenberg 2D lattice (top continuous line) and for a regular Heisenberg chain (bottom continuous line) aiming at matching the position of the maximum of susceptibility are plotted in Figure 3. Values of J equals to -1.4 and -3.2 cm^{-1}, respectively, are required for that. Therefore, the values of J involved in the alternating plane (J_{bpm} and J_{ox}) should be between these two values, in agreement with those obtained for compounds **1** and **4**.

To conclude, this work shows how the polymerization through bischelating ligands such as bpm and ox using suitable precursors (either mononuclear Cu(bpm)(ox) or dinuclear $[Mn_2(bpm)]^{4+}$ species) as building blocks provides us with a new strategy to design novel honeycomb layered materials.

Acknowledgment. This work was supported by the Spanish DGICYT (Project PB91-0807-C02-01), the Italian Ministero dell'Università e della Ricerca Scientifica e Tecnologica, and the Human Capital and Mobility Program (Network on Magnetic Molecular Materials from EEC) through Grant ERBCHRX-CT920080. R.R. also thanks the Conselleria de Cultura, Educació i Ciència de la Generalitat Valenciana, for a predoctoral fellowship.

Supplementary Material Available: Tables listing crystal data, hydrogen atom coordinates, intramolecular bond distances and angles, hydrogen-bonding parameters, and least-squares planes for **1** and **2** and a figure showing the thermal dependence of the molar magnetic susceptibility for **1** (13 pages). Ordering information is given on any current masthead page.

IC940280H

(11) Deguenon, D.; Bernardelli, G.; Tuchagues, J. P.; Castan, P. *Inorg. Chem.* **1990**, *29*, 3031.

(12) Navarro, R. In *Magnetic Properties of Layered Transition Metal Compounds*; de Jongh, J. J., Ed.; Kluwer Academic Publishers: Dordrecht, The Netherlands, 1990; Vol. 9.

(13) Wagner, G. R.; Friedberg, S. A. *Phys. Lett.* **1964**, *9*, 11. Fisher, M. E. *Am. J. Phys.* **1964**, *32*, 343. König, E.; Desai, V. P.; Kanellakopoulus, B.; Klenze, R. *Chem. Phys.* **1980**, *54*, 109.